Li Diffusion in Li_xCoO_2 Probed by Muon-Spin Spectroscopy

Jun Sugiyama,[1,*] Kazuhiko Mukai,[1] Yutaka Ikedo,[1,†] Hiroshi Nozaki,[1] Martin Månsson,[2] and Isao Watanabe[3]
[1]Toyota Central Research and Development Laboratories Inc., Nagakute, Aichi 480-1192 Japan
[2]Laboratory for Neutron Scattering, ETH Zürich and Paul Scherrer Institut, CH-5232 Villigen PSI, Switzerland
[3]Muon Science Laboratory, RIKEN, 2-1 Hirosawa, Wako, Saitama 351-0198, Japan

(Received 16 June 2009; published 30 September 2009)

The diffusion coefficient of Li^+ ions (D_{Li}) in the battery material Li_xCoO_2 has been investigated by muon-spin relaxation (μ^+SR). Based on experiments in zero and weak longitudinal fields at temperatures up to 400 K, we determined the fluctuation rate (ν) of the fields on the muons due to their interaction with the nuclear moments. Combined with susceptibility data and electrostatic potential calculations, clear Li^+ ion diffusion was detected above ~150 K. The D_{Li} estimated from ν was in very good agreement with predictions from first-principles calculations, and we present the μ^+SR technique as an optimal probe to detect D_{Li} for materials containing magnetic ions.

DOI: 10.1103/PhysRevLett.103.147601 PACS numbers: 76.75.+i, 66.30.H−, 82.47.Aa, 82.56.Lz

In spite of a long research history on lithium insertion materials for Li-ion batteries [1], e.g., $LiCoO_2$, $LiNiO_2$, and $LiMn_2O_4$, one of their most important intrinsic physical properties, the Li^+ ions diffusion coefficient (D_{Li}), has not yet been determined with any reliability. Although Li NMR is a powerful technique to measure D_{Li} for nonmagnetic materials, it is particularly difficult to evaluate D_{Li} for materials containing magnetic ions, because the magnetic ions induce additional pathways for the spin-lattice relaxation rate ($1/T_1$), resulting in huge $1/T_1$ compared with that expected for only the diffusive motion of Li ions.

Such difficulty was clearly evident in the $1/T_1(T)$ curve for $LiCoO_2$ and $LiNiO_2$ [2,3], and, for that reason, D_{Li} was instead estimated from the Li NMR linewidth [4]. However, since the linewidth, i.e., the spin-spin relaxation rate ($1/T_2$), is also affected by the magnetic ions, the D_{Li} obtained by Li NMR for $LiCoO_2$ ($= 1 \times 10^{-14}$ cm^2 s^{-1} at 400 K) is approximately 4 orders of magnitude smaller than predicted by first-principles calculations [5]. Since lithium insertion materials always include transition metal ions, in order to maintain charge neutrality during the extraction and/or insertion of Li^+ ions, it is consequently very difficult to determine D_{Li} for these compounds unambiguously by Li NMR.

On the other hand, the chemical diffusion coefficient (D_{Li}^{chem}), which is measured under a potential gradient, has also been determined by electrochemical measurements. Note that the relationship between D_{Li} and D_{Li}^{chem} is given by $D_{Li}^{chem} = \Theta D_{Li}$, where Θ is a thermodynamic factor. The magnitude of D_{Li}^{chem} is, however, known to be very sensitive to the measurement system, e.g., the electrolyte as well as the compositions of the positive and negative electrodes. As a result, the reported D_{Li}^{chem} for Li_xCoO_2 ranges from 4×10^{-8} to 10^{-10} cm^2 s^{-1} for powder samples [6–10] and from 2.5×10^{-11} to 2×10^{-13} cm^2 s^{-1} for thin films [11–14] at ambient T. In order to profoundly understand the physics behind the operation principle of battery materials, it is imperative to have a reliable probe to measure D_{Li} for all the components of the battery as a function of both Li content as well as T. This is at present a key issue for further development of Li-ion batteries, and, in particular, for future fabrication of solid-state batteries.

In contrast to NMR, the effect of localized moments in a paramagnetic (PM) state on the muon-spin relaxation (μ^+SR) signal is very limited at high T, because the PM fluctuation is usually too fast to be visible by μ^+SR. Furthermore, although μ^+SR is very sensitive to the local magnetic environment, whether it is due to electronic or nuclear spins, an electronic contribution is, in principle, distinguishable from a nuclear contribution by weak longitudinal field measurements. In addition, since the μ^+SR time scale is different from the NMR's time scale, μ^+SR is expected to provide unique information on nuclear magnetic fields. Indeed, μ^+SR studies of Li_xCoO_2 at low T indicate that μ^+'s *feel* a nuclear magnetic field caused by Li and ^{59}Co even at 1.8 K [15,16]. This offers a possibility to determine D_{Li} of Li_xCoO_2 by μ^+SR, if μ^+'s locate in the vicinity of the O^{2-} ion and make a stable μ^+-O^{2-} bond in the Li_xCoO_2 lattice. Here, we report our initial work on Li_xCoO_2 ($x = 0.73$ and 0.53) to estimate their D_{Li} and establish μ^+SR as a novel tool to probe Li-ion diffusion.

A powder sample of $LiCoO_2$ was prepared at Osaka City University by a solid-state reaction technique using reagent grade $LiOH \cdot H_2O$ and $CoCO_3$ powders as starting materials. A mixture of the two powders was heated at 900 °C for 12 h in air. Powder x-ray diffraction (XRD) analysis showed that the $LiCoO_2$ sample was single phase with a rhombohedral system of space group $R\bar{3}m$ ($a_H = 0.2814$ nm and $c_H = 1.4049$ nm in hexagonal setting). The Li-deficient samples were prepared by an electrochemical reaction using Li | $LiPF_6$-ethylene carbonate-diethyl carbonate | $LiCoO_2$ cells. The $LiCoO_2$ powder was pressed into a disk with 15 mm diameter and 0.4 mm thickness, and the disk was then used as a positive electrode. The Li_xCoO_2 disk was removed from the cell in a glovebox and packed into a sealed powder cell just before the μ^+SR measurement. Their structures were subsequently confirmed by powder XRD, and, finally, their compositions were checked by an inductively coupled plasma atomic emission spectral analysis. The above procedure is essentially the same as that of our previous μ^+SR work on Li_xCoO_2 [16] and Li_xNiO_2 [17].

The μ^+SR spectra were measured at the surface muon beam line of the RIKEN-RAL Muon Facility at ISIS (U.K.) using a liquid-He flow-type cryostat in the T range between 10 and 400 K. The experimental techniques were described elsewhere [18]. χ was measured using a SQUID magnetometer (MPMS, Quantum Design) in the T range between 5 and 200 K under a magnetic field of $H = 100$ Oe.

Figure 1 shows the zero field (ZF) and longitudinal field (LF) μ^+SR spectrum for the $Li_{0.73}CoO_2$ sample obtained at 100 and 225 K. At 100 K, the ZF spectrum exhibits a typical Kubo-Toyabe (KT) behavior with a minimum at $t \sim 6$ μs, meaning that the implanted muons *see* the internal magnetic field ($H_{\rm int}$) due to the nuclear magnetic moments of ^{7}Li, ^{6}Li, and ^{59}Co. The applied LF clearly reduces the relaxation rate, i.e., the time slope, by decoupling $H_{\rm int}$. Although the ZF spectrum still shows KT behavior at 225 K, the relaxation rate is smaller than at 100 K.

In order to estimate the KT parameters precisely, the ZF and two LF spectra were fitted simultaneously by a combination of a dynamic Gaussian KT function $[G^{\rm DGKT}(\Delta, \nu, t, H_{\rm LF})]$ and a background (BG) signal from the fraction of muons stopped mainly in the sample holder, which is made of high-purity aluminum;

$$A_0 P_{\rm LF}(t) = A_{\rm KT} G^{\rm DGKT}(\Delta, \nu, t, H_{\rm LF}) + A_{\rm BG}, \qquad (1)$$

where A_0 is the initial ($t = 0$) asymmetry, $A_{\rm KT}$ and $A_{\rm BG}$ are the asymmetries associated with the two signals. Δ is the static width of the local field distribution at the disordered sites, and ν is the field fluctuation rate. When $\nu = 0$ and $H_{\rm LF} = 0$, $G^{\rm DGKT}(t, \Delta, \nu, H_{\rm LF})$ is the static Gaussian KT function $G_{zz}^{\rm KT}(t, \Delta)$ in ZF. At first, we fitted all the ZF spectra using common $A_{\rm KT}$ and $A_{\rm BG}$ in Eq. (1). The "global fit" provided that $A_{\rm KT} = 0.164\,06 \pm 0.000\,02$ (0.1689 ± 0.0002) and $A_{\rm BG} = 0.063\,50 \pm 0.000\,02$ (0.0692 ± 0.0002) for $Li_{0.73}CoO_2$ ($Li_{0.53}CoO_2$). Then, using the obtained $A_{\rm KT}$ and $A_{\rm BG}$, one ZF and two LF spectra were global-fitted using common Δ and ν at each T.

Figure 2 shows the T dependencies of both Δ and ν for the two samples together with χ measured in a 100 Oe magnetic field. For $Li_{0.73}CoO_2$, Δ is almost constant for $5 \le T \le 250$ K, indicating that the μ^+ are most probably stable in the crystal lattice until ~300 K. Δ then rapidly decreases, but levels off again for $T \ge 325$ K. The $\nu(T)$ curve is almost T-independent up to 150 K, starts to increase at ~150 K, and exhibits a maximum at 275 K. Above 275 K, ν decreases to 0.7×10^6 s^{-1} at ~325 K, and finally becomes almost T-independent above 350 K. The increase in ν between 150 and 275 K is well explained by a thermal activation process [Figs. 2(g) and 2(h)], which signals the onset of diffusive motion of either Li$^+$ or μ^+ above 150 K. The clear decrease in Δ at ~300 K also suggests an additional diffusion of Li$^+$ or μ^+.

The $\chi(T)$ curve exhibits a small anomaly around 150 K with a thermal hysteresis of ~10 K, while there is no indication of any magnetic anomalies in the T range between 200 and 300 K [Figs. 2(e) and 2(f)] [15,16]. This suggests that the change in the μ^+SR parameters around 150 K is caused by an intrinsic change in Li_xCoO_2, but the change around 300 K is visible only by μ^+SR. The increase in ν above 150 K is, thus, most unlikely due to μ^+ diffusion, but it is rather due to Li$^+$ diffusion; i.e., either a freezing of the Li$^+$ motion or an order-disorder transition of the Li+ ions occurs below around 150 K. This is also supported by a recent ^{7}Li NMR experiment [19], in which the NMR linewidth-versus-T curve for $Li_{0.6}CoO_2$ exhibits a steplike decrease with T around 150 K by motional narrowing due to Li$^+$ diffusion. Since such diffusion naturally increases a local structural symmetry, it is reasonable that Δ slightly decreases with T around 150 K. On the other hand, both Li$^+$ and μ^+ are inferred to be diffusing above 300 K, resulting in the large decrease in Δ caused by motional narrowing. Actually, because $\Delta \le 0.1\nu$ above 300 K, Eq. (1) is roughly equivalent to an exponential relaxation function $[\exp(-\lambda t)]$, and it is difficult to estimate Δ and ν precisely at high T.

The result for the $Li_{0.53}CoO_2$ sample is very similar to that of $Li_{0.73}CoO_2$, although $\Delta_{T\to 0}(Li_{0.53}CoO_2) < \Delta_{T\to 0}(Li_{0.73}CoO_2)$ due to the decrease in the number den-

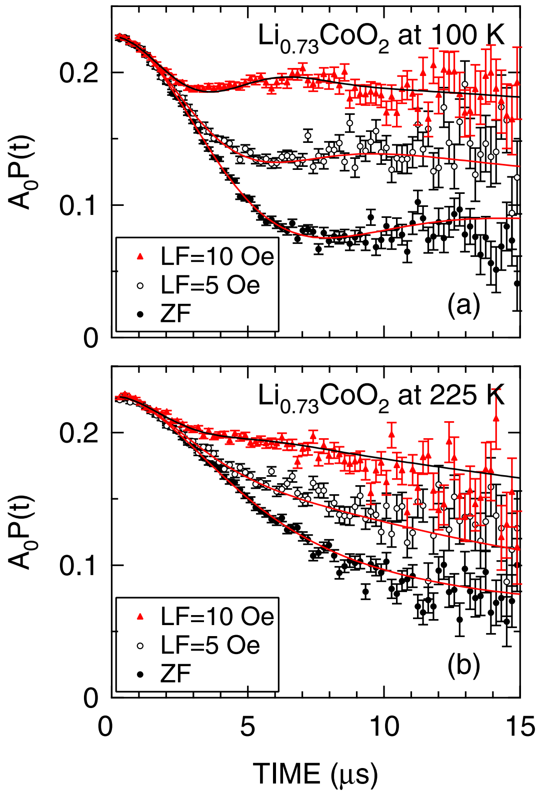

FIG. 1 (color online). ZF and two LF μ^+SR spectra for $Li_{0.73}CoO_2$ measured at (a) 100 K and (b) 225 K. Solid lines represent the fit result using Eq. (1).

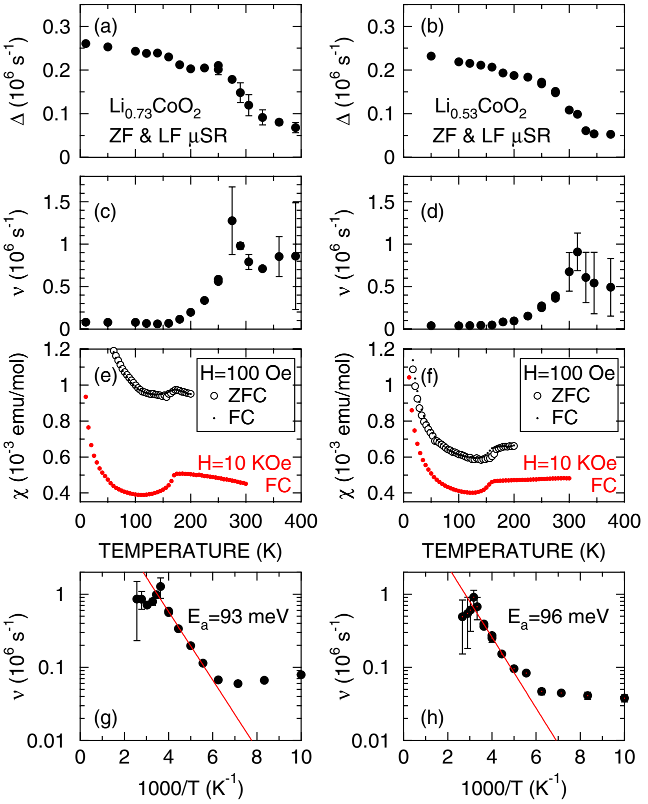

FIG. 2 (color online). For $Li_{0.73}CoO_2$ and $Li_{0.53}CoO_2$, respectively, we show T dependences of (a),(b) field distribution width (Δ), (c),(d) field fluctuation rate (ν), (e),(f) susceptibility (χ), and (g),(h) the log(ν)-vs-$1/T$ curve. Δ and ν were obtained by fitting both ZF and LF spectra using Eq. (1). χ was measured in both field cooling (FC) and zero field cooling (ZFC) mode with $H = 100$ Oe. In (e),(f), the χ data [16] measured in FC mode with $H = 10$ kOe for $Li_{0.75}CoO_2$ and $Li_{0.52}CoO_2$ were also plotted for comparison. The straight lines in (g) and (h) show the activated diffusive behavior discussed in the text.

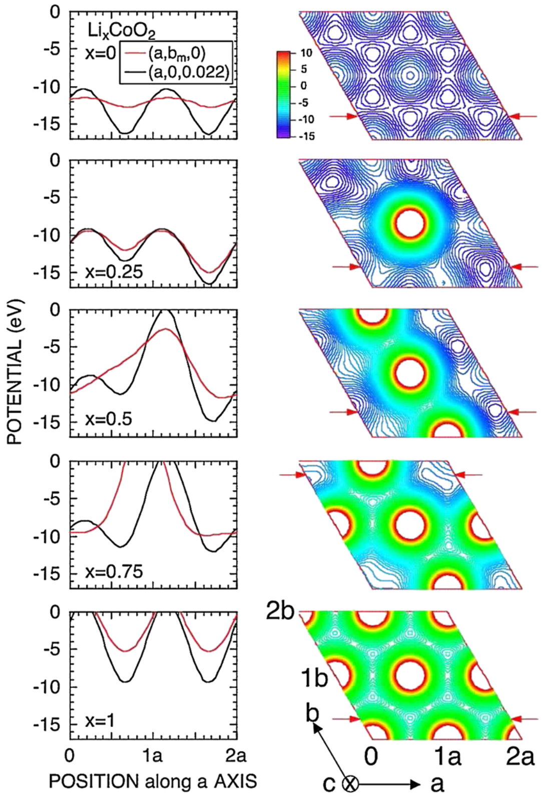

FIG. 3 (color online). The variation of electrostatic potential (ϕ_E) along the a axis at $b = b_m$ and $c = 0$ (on the Li plane) and $b = 0$ and $c = 0.022$ (1 Å away from the O^{2-} ions) in the hexagonal lattice of Li_xCoO_2 with $x = 0$, 0.25, 0.5, 0.75, and 1 (from top to bottom). Here, b_m denotes the b, at which electrostatic potential exhibits a minimum. The right-hand panels show the corresponding distribution of ϕ_E in the Li plane. Arrows on the b axis in the right-hand panels represents b_m.

sity of Li^+ ions, as reported previously [15,16]. Also, the magnitude of ν of $Li_{0.53}CoO_2$ is smaller than ν of $Li_{0.73}CoO_2$ in the whole T range measured, but the $\nu(T)$ curve for both samples shows a clear increase with T above 150 K and a maximum around 300 K.

In order to predict the muon site(s) and to confirm the reliability of the above assumption that Li^+ ions diffuse above 150 K whereas μ^+ diffuse only above 300 K, we performed electrostatic potential (ϕ_E) calculations for the Li_xCoO_2 lattice using a point-charge model and the program DIPELEC [20]. As seen in Fig. 3, the site in the vicinity of the O^{2-} ions is more stable for μ^+ than the site in the Li plane for the whole x range between 1 and 0. This means that μ^+'s are bound to the O^{2-} ions so as to make a stable μ^+-O^{2-} bond in Li_xCoO_2. This is a common situation in oxides, as, for example, in the case for the high-T_c cuprates [21]. Since μ^+'s are assigned as an ideal point charge, such a μ^+-O^{2-} bond should be purely ionic. In fact, dipole field calculations for the site in the vicinity of the O^{2-} ions provide that $\Delta_{\rm calc} = 0.43 \times 10^6$ s^{-1} (0.35×10^6 s^{-1}) for Li_xCoO_2 with $x = 3/4$ (1/2). Furthermore, $\Delta_{\rm calc}$ is found to be comparable to Δ measured at low T in the whole x range for Li_xCoO_2 [16], if we consider the reduction of Δ by the electric field gradient effect on the nuclear moments with $I \geq 1$ [22,23]. This suggests that the point-charge model is acceptable for determining the muon site(s) in Li_xCoO_2. As a result, it is clarified that, as T increases from 5 K, the Li^+ ions start to diffuse above 150 K ($= T_d^{\rm Li}$) and then the μ^+ diffuse above 300 K ($= T_d^{\mu}$), in spite of the mass difference between μ^+ and Li^+ ($m_{Li^+}/m_{\mu^+} \sim 63$) because the muons form a hydrogenlike bond with oxygen.

Finally, we estimate $D_{\rm Li}$ using the obtained fluctuation rate ν as directly measuring the jump rate. Figure 4(a) shows the possible jump paths for the Li ions, i.e., the direct jump to the nearest (vacant) Li site (path number 1) and the jump to the interstitial site in the center of the oxygen tetrahedron (path number 2). Assuming that ν corresponds to the jump rate of the Li ions between the neighboring sites, $D_{\rm Li}$ is given by [24]

$$D_{\rm Li} = \sum_{i=1}^{n} \frac{1}{N_i} Z_{v,i} s_i^2 \nu, \qquad (2)$$

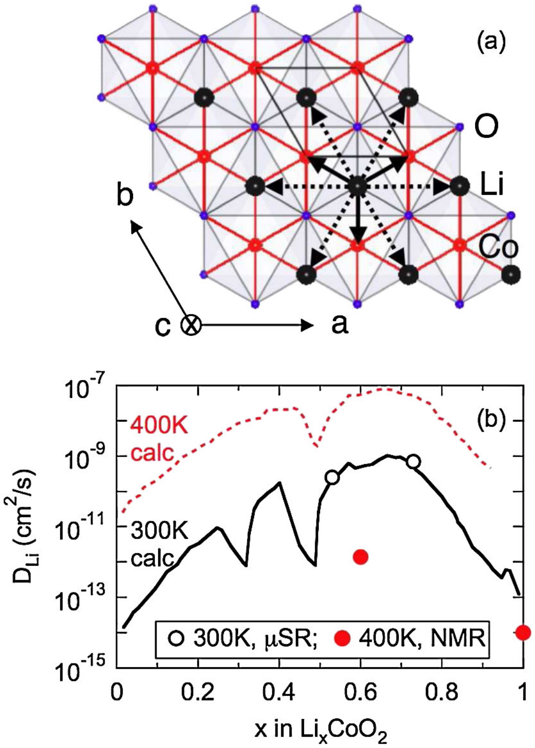

FIG. 4 (color online). (a) Possible jump paths for Li ions. Broken arrows represent the direct jump to nearest (vacant) Li site (path number 1), whereas solid arrows represent the jump to an interstitial site in the center of the oxygen tetrahedron (path number 2). (b) The relationship between D_{Li} and x in $\mathrm{Li}_x\mathrm{CoO}_2$ as extracted from our μ^+SR experiment (open circles). The solid line and the dashed line represent the predictions by first-principles calculations [5] at $T = 300$ and 400 K, respectively, when the effective vibration frequency is a typical value (10^{13} s^{-1}). Sharp minima in the predicted curve (at $x = 1/3$ and $1/2$) are caused by Li ordering. The ^{7}Li NMR result [4,19] for $T = 400$ K is also plotted (solid dot) for comparison.

where N_i is the number of Li sites in the ith path, $Z_{v,i}$ is the vacancy fraction, and s_i is the jump distance. Here, we naturally restrict the path to lie in the c plane, i.e., along the 2D channel, because it is most unlikely that the Li ions jump across the CoO_2 plane to an adjacent Li plane. Therefore, $N_1 = 6$, $N_2 = 3$, s_1 is equivalent to the a-axis length, $s_2 = a/\sqrt{3}$, $Z_{v,1} = 0.27$ for $\mathrm{Li}_{0.73}\mathrm{CoO}_2$ (0.47 for $\mathrm{Li}_{0.53}\mathrm{CoO}_2$), and $Z_{v,2} = 1$. As a result, we obtain $D_{\mathrm{Li}} = (7 \pm 2) \times 10^{-10}$ cm^2/s $[(2.5 \pm 0.8) \times 10^{-10}$ $\mathrm{cm}^2/\mathrm{s}]$ for $\mathrm{Li}_{0.73}\mathrm{CoO}_2$ $[\mathrm{Li}_{0.53}\mathrm{CoO}_2]$ at 300 K. Here, $\nu(300\ \mathrm{K})$ for $\mathrm{Li}_{0.73}\mathrm{CoO}_2$ was estimated from the extrapolation of the linear relationship between $\log[\nu]$ and T^{-1} [see Fig. 2(g)]. The estimated D_{Li} is found to be very consistent with the prediction by first-principles calculations [5], as seen in Fig. 4(b). Note that the jump paths used in Eq. (2) are the same as those for the first-principles calculations. This means that there is no ambiguous factor for estimating D_{Li} by μ^+SR. Since μ^+SR detects ν ranging from $\sim 0.01\Delta$ to $\sim 10\Delta$, it is applicable for materials with $D_{\mathrm{Li}} = 10^{-12}$–$10^{-9}$ cm^2/s, when $N = 10$, $Z_v = 1$, $s = 1$ nm, and $\Delta = 0.1 \times 10^6$ s^{-1}.

In conclusion, we have been able to determine the Li diffusion coefficient, D_{Li}, of $\mathrm{Li}_x\mathrm{CoO}_2$ from the fluctuation rate of the field experienced by the muons in interaction with the nuclear moments of the diffusing ions. The value was found to be in good agreement with theoretical predictions. Consequently, we would like to suggest μ^+SR as a novel probe to investigate Li diffusion, especially for materials containing transition metal ions.

This work was performed at the RIKEN-RAL Muon Facility at ISIS, and we thank the staff for help with the μ^+SR experiments. We appreciate T. Ohzuku and K. Ariyoshi for sample preparation and K. Yoshimura for discussion. J. S. and Y. I. are supported by the KEK-MSL Inter-University Program for Overseas Muon Facilities. This work is also supported by Grant-in-Aid for Scientific Research (B), 19340107, MEXT, Japan.

---

[*] e0589@mosk.tytlabs.co.jp

[†] Present address: Muon Science Laboratory, Institute of Materials Structure Science, High Energy Accelerator Research Organization, Tsukuba, Japan.

[1] T. Ohzuku and R. Brodd, J. Power Sources **174**, 449 (2007).
[2] I. Tomeno and M. Oguchi, J. Phys. Soc. Jpn. **67**, 318 (1998).
[3] K. Nakamura *et al.*, Solid State Ionics **121**, 301 (1999).
[4] K. Nakamura *et al.*, Solid State Ionics **135**, 143 (2000).
[5] A. Van der Ven and G. Ceder, Electrochem. Solid-State Lett. **3**, 301 (2000).
[6] K. Mizushima *et al.*, Solid State Ionics **3–4**, 171 (1981).
[7] C. Y. Yao *et al.*, J. Power Sources **54**, 491 (1995).
[8] S.-Il Pyun and Y.-M. Choi, J. Power Sources **68**, 524 (1997).
[9] K. Dokko *et al.*, J. Electrochem. Soc. **148**, A422 (2001).
[10] K. Dokko *et al.*, J. Power Sources **189**, 783 (2009).
[11] K. A. Striebel *et al.*, J. Electrochem. Soc. **143**, 1821 (1996).
[12] Y. H. Rho and K. Kanamura, J. Electrochem. Soc. **151**, A1406 (2004).
[13] H. Xia *et al.*, J. Electrochem. Soc. **154**, A337 (2007).
[14] S. B. Tang *et al.*, J. Alloys Compd. **449**, 300 (2008).
[15] J. Sugiyama *et al.*, Phys. Rev. B **72**, 144424 (2005).
[16] K. Mukai *et al.*, Phys. Rev. Lett. **99**, 087601 (2007).
[17] J. Sugiyama *et al.*, Phys. Rev. B **78**, 144412 (2008).
[18] G. M. Kalvius *et al.*, in *Handbook on the Physics and Chemistry of Rare Earths*, edited by K. A. Gschneidner *et al.* (Elsevier Science, Amsterdam, 2001), Vol. 32, Ch. 206, and references cited therein.
[19] K. Nakamura *et al.*, Solid State Ionics **177**, 821 (2006).
[20] K. M. Kojima *et al.*, Phys. Rev. B **70**, 094402 (2004).
[21] T. R. Adams *et al.*, Hyperfine Interact. **86**, 561 (1994).
[22] R. S. Hayano *et al.*, Phys. Rev. B **20**, 850 (1979).
[23] C. T. Kaiser *et al.*, Phys. Rev. B **62**, R9236 (2000).
[24] R. J. Borg and G. J. Dienes, *An Introduction to Solid State Diffusion* (Academic, San Diego, 1988).